

Development of Dynamic Model of Autonomous Sailboat for Simulation and Control

Joga Dharma Setiawan^{1,2}

¹Mechanical Engineering Department
Universitas Diponegoro
Semarang, Indonesia

²National Center for Sustainable
Transportation Technology, Indonesia
joga.setiawan@ft.undip.ac.id

Deddy Chrismianto

Naval Architecture Department
Universitas Diponegoro
Semarang, Indonesia
deddychrismianto@yahoo.co.id

Mochammad Ariyanto^{1,2}

¹Mechanical Engineering Department
Universitas Diponegoro
Semarang, Indonesia

²National Center for Sustainable
Transportation Technology, Indonesia
mochammad_ariyanto@ft.undip.ac.id

Candra Wahyu Sportyawan^{1,2}

¹Mechanical Engineering Department
Politeknik Negeri Bandung

²Mechanical Engineering Department
Universitas Diponegoro
Semarang, Indonesia
candrawahyus.mesin@gmail.com

Robby Dwianto Widyantara

Mechanical Engineering Department
Universitas Diponegoro
Semarang, Indonesia
robbydwianto@gmail.com

Sabri Alimi

Center for Biomechanics Biomaterial
Biomechatronics and Biosignal
Processing
Universitas Diponegoro
Semarang, Indonesia
alimi.sabr@gmail.com

Abstract— An autonomous sailboat is a robotic boat that utilizes wind energy as a booster with the ability to control its sails and steering without human intervention. An autonomous sailboat can be used for monitoring the ocean with realtime data collection and relatively easy and affordable installation. Therefore research on autonomous sailboats is important, especially for Indonesia, which has an extensive area of ocean. In this study, the autonomous boat uses wing sail with flap and rudder to produce propulsion. The simulation model of an autonomous sailboat dynamic with 4-DOF was created using MATLAB/Simulink. Simulations were carried out to determine the effect of flap and rudder deflection angles on boat dynamics. The objective of this study is reveal the primary characteristics of boat sailboat dynamic such that the four direction combinations of the flap and rudder can steer the sailboat to the desired motion. Thus, the simulation model can be useful in formulating the in-progress control algorithm for the autonomous boat.

Keywords— Ocean monitoring, autonomous sailboat, dynamic simulation.

I. INTRODUCTION

An autonomous sailboat is a robotic boat that utilizes wind energy to get thrust and can control its sails and steering without human intervention [1]. An autonomous sailboat is used as a monitoring or data collection platform in the ocean because of its advantages which can carry many sensors, send data in realtime, and its relatively easy installation. An autonomous boat moves using the control input determined by an algorithm based on environmental conditions and the destination point data. To develop the algorithm, the boat's dynamic response to control inputs under an environmental condition needs to be well known.

Mechanically, an autonomous boat interacts with two fluids: air and water, at which the relative motion between the boat with the air and water produces aerodynamic and hydrodynamic forces, respectively [2]. In this study, an autonomous boat simulation model was created to predict the dynamic response of the boat by varying the deflection of the flap angle (δ_f) and the rudder angle. The flap controls the wing

angle of attack (α). This study assumes that the wind blows from one direction at a constant speed and the state of seawater state is calm. Further, for the sake of simplicity, the dynamic of the boat is developed using 4-DOF model.

II. METHODS OF WING SAILING AND SIMULATION

A. Wing Sail Autonomous Boat

The boat has main components that are hull, wingsail, flap, and rudder, as shown in Figure 1.

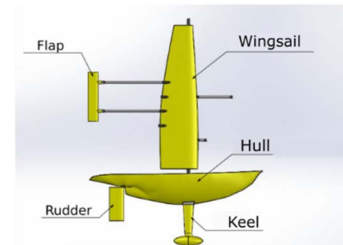


Fig. 1. Wing sail autonomous boat main components

The boat hull provides buoyancy and storage for other components such as sensors, frames, and batteries. The hull is equipped with a keel that serves as a stabilizer for rotation movement in the roll axis. The airfoil-shaped wing sail serves to produce the thrust of the boat when interacting with the wind. The angle of attack of the wing sails against the wind is set using the flap deflection. For turning and maneuvering, the autonomous boat uses a rudder. A control input controls flap and rudder deflections.

B. Dynamics of Sailing

For ease of modeling and dynamic analysis, a body coordinate system and a global coordinate system are created, as in Legursky [3]. The body and global coordinate systems are shown in Figure 2.

The wing sail, flap, and rudder working principles are such as aircraft wings where the wing produces aerodynamic forces, lift (L) and drag (D) from the fluid that passes through

it [4]. The wing sail, flap, and rudder use the NACA0018 type airfoil. The relationship between lift and drag coefficients to the angle of attack of the NACA0018 airfoil was taken from Du [5]. The convention of the wing sail angle of attack, flap, and rudder deflection angle are shown in Figure 3.

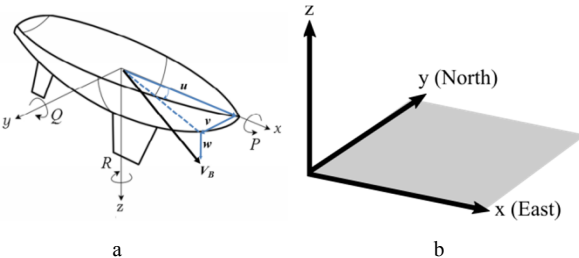


Fig. 2. Coordinate systems a) body , b) global

where

$$\begin{aligned} u &= \text{surge velocity (m/s)} & \Phi &= \text{roll angle (rad)} \\ v &= \text{sway velocity (m/s)} & \theta &= \text{pitch angle (rad)} \\ w &= \text{heave velocity (m/s)} & \psi &= \text{yaw angle (rad)} \\ P &= \text{roll angular velocity (rad/s)} \\ Q &= \text{pitch angular velocity (rad/s)} \\ R &= \text{yaw angular velocity (rad/s)} \end{aligned}$$

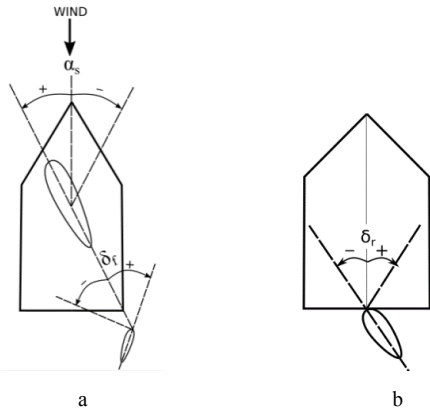


Fig. 3. Convention of a) wing sail angle of attack and flap deflection angle, b) rudder deflection angle

The angle of attack of the wing sail with respect to the wind is set using the moment produced by the flap by its deflection. The effect of flap deflection on the angle of attack of the wing sail was obtained from Tretow [2] using (1).

$$\alpha_s = \delta_f \times 3.21 \quad (1)$$

When the boat moves, there is relative movement between the boat and the wind, so the direction of the wind that wing sail receives is different from the absolute wind direction. The relative wind direction received by the wing sail hereafter is called apparent wind. So the angle of attack of the wing sail is measured from the direction of the apparent wind. Boat velocity (v_b), absolute wind velocity (v_t), and apparent wind velocity (v_p) are illustrated in Figure 4 in which the boat velocity is defined by (2) and (3), and the convention is shown in Figure 5.

$$v_b = \sqrt{u^2 + v^2} \quad (2)$$

$$\gamma = \tan^{-1} \left(\frac{v}{u} \right) \quad (3)$$

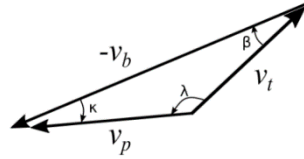


Fig. 4. Apparent wind (v_p)

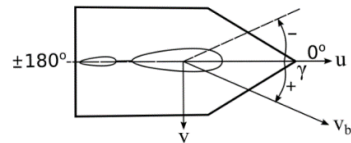


Fig. 5. Boat velocity convention

The forces and moments generated by the wing sail are transformed into the body coordinates become wing sail forces on the x-axis (X_s), forces on the y-axis (Y_s), and roll moments (K_s) defined by (4) to (6).

$$X_s = -L_s \cdot \sin((\varphi - \lambda) + \psi) + D_s \cdot \cos((\varphi - \lambda) + \psi) \quad (4)$$

$$Y_s = -L_s \cdot \cos((\varphi - \lambda) + \psi) + D_s \cdot \sin((\varphi - \lambda) + \psi) \quad (5)$$

$$K_s = Y_s \cdot d_{zs} \quad (6)$$

where L_s is the wing sail lift force, D_s is the wing sail drag force, φ is the angle of the absolute wind to East, λ is the angle of the absolute wind to the apparent wind, and d_{zs} is the distance of the wing sail force point of action to the boat's center of rotation on the Z-axis.

As in the wing sail, the rudder produces the hydrodynamic force, lift (L_r) and drag (D_r) from water that moves relatively through it. The forces and moments generated by rudder are transformed into the body coordinates and become rudder forces on the x-axis (X_r), forces on the y-axis (Y_r), roll moment (K_r), and yaw moment (N_r) defined by (7) to (10).

$$X_r = L_r \cdot \sin(\gamma) - D_r \cdot \cos(\gamma) \quad (7)$$

$$Y_r = -L_r \cdot \cos(\gamma) - D_r \cdot \sin(\gamma) \quad (8)$$

$$K_r = Y_r \cdot (-d_{zr}) \quad (9)$$

$$N_r = Y_r \cdot (-d_{xr}) \quad (10)$$

where γ is the angle of boat velocity, d_{zr} is the distance of the rudder force point action to the center of rotation of the boat on the x-axis, d_{xr} is the distance of the rudder force point action to the center of rotation of the boat on the x-axis. Using (11) to (18) [6] a boat acceleration is obtained from the resultant of wing sail and rudder forces and moments.

$$\dot{u} = \frac{X}{m} + vR \quad (11)$$

$$\dot{v} = \frac{Y}{m} - uR \quad (12)$$

$$\dot{P} = \frac{I_{zz}K + I_{xz}N}{I_{xx}I_{zz} - I_{xz}^2} \quad (13)$$

$$\dot{R} = \frac{I_{xx}N + I_{xz}K}{I_{xx}I_{zz} - I_{xz}^2} \quad (14)$$

$$X = X_s + X_r + X_{drag} \quad (15)$$

$$Y = Y_s + Y_r + Y_{drag} \quad (16)$$

$$K = K_s + K_r + K_{drag} \quad (17)$$

$$N = N_r + N_{drag} \quad (18)$$

where I is the inertia of the boat, m is the mass of the boat, X is the total external force on the x -axis of the boat, Y is the total external force on the y -axis, K is the total external moment on the roll axis, and N is the total external moment on the yaw axis. Then boat velocity in global coordinates is calculated using (19) and (20).

$$\dot{x} = u \cdot \cos(-\psi) + v \cdot \sin(-\psi) \quad (19)$$

$$\dot{y} = u \cdot \sin(-\psi) - v \cdot \cos(-\psi) \quad (20)$$

C. Dynamics Simulation Model

The autonomous boat dynamics are simulated using MATLAB Simulink and modeled with 3D Animation. The Simulink blocks are divided into five parts; wing sail, rudder, body, Simulink signal conversion into 3D animation input, and 3D block animation, as shown in Figure 6. The simulation uses the main parameters shown in Table I.

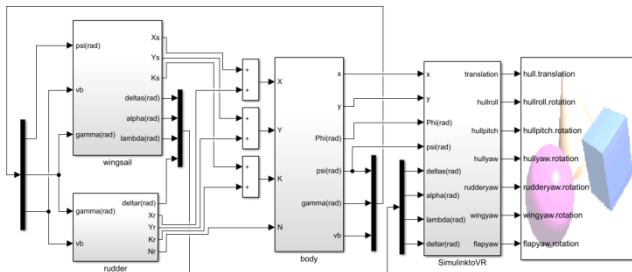


Fig. 6. Dynamics model in Simulink

TABLE I. MAIN PARAMETERS FOR SIMULATION

Parameter	Unit	Value
Air Density	kg/m ³	1.25
Wind velocity from the East	m/s	5
Sail planform area	m ²	0.5069
Rudder planform area	m ²	0.0525
Water density	kg/m ³	1025
Boat mass	kg	25.5
I_{xx} of boat	kg.m ²	0.265
I_{xz} of boat	kg.m ²	0.004
I_{zz} of boat	kg.m ²	0.013

D. Simulation Setup

The dynamics analysis of the wing sail autonomous boat is done by simulating the boat for 100 seconds by varying the input of flap deflection (δ_f), which regulates the wing sail angle of attack (α_s) and the input of rudder deflection (δ_r). The boat is initially still and faces the positive x -axis in global coordinates ($\psi = 0$). The wind blows at a constant speed of 5 m/s to West or negative X -axis in global coordinates ($\phi = 0$). The list of cases of wing sail autonomous boat simulation is shown in Table II.

III. SIMULATION RESULTS AND ANALYSIS

A. Case I

In the first case the flap and rudder are not deflected ($\delta_f = 0$ and $\delta_r = 0$) until the end of the simulation. The undeflected flap ($\delta_f = 0^\circ$) makes the angle of attack of the wing sail $\alpha_s = 0^\circ$ so that the wing sail only produces drag force that pushes the boat back. Due to the boat moving backward, there is relative motion between the rudder and seawater which makes the rudder produce drag force towards the front of the boat. The

free-body diagram at the beginning of the simulation of case I is shown in Figure 7.

TABLE II. LIST OF CASES FOR SIMULATION

Case	Rudder angle, δ_r ($^\circ$)	Flap angle, δ_f ($^\circ$)	Wing sail angle of attack, α_s ($^\circ$)
I	0	0	0
II	0	-4 → 4 (inc. 1°)	-12.8 → 12.8
III	15	4	12.8
IV	-15	4	12.8
V	-15 → 15 (square wave)	4 → -4 (square wave)	12.8 → -12.8

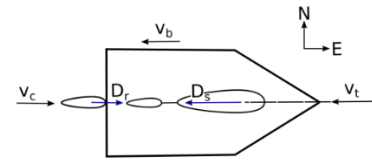


Fig. 7. Free-body diagram at the beginning of case I, $\delta_f = 0^\circ$ and $\delta_r = 0^\circ$

At the beginning of the simulation the boat moves backward parallel to the x -axis in the negative x -axis direction. After 12 seconds, the boat starts rotating counter-clockwise, as shown in Figure 8.

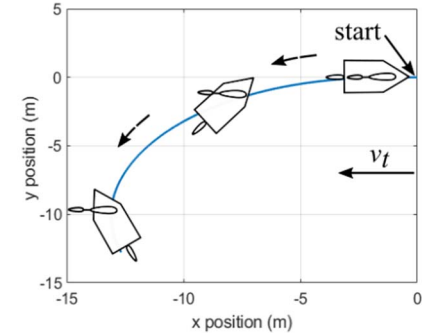


Fig. 8. Boat movement in case I, $\delta_f = 0^\circ$ and $\delta_r = 0^\circ$

In case I, the boat velocity reaches a maximum value of 0.29 m/s with the direction of the boat velocity around the angle of -180° or towards the back of the boat.

B. Case II

In case II the rudder is not deflected ($\delta_r = 0$), and flap deflection (δ_f) is varied in the angle range of -4° to 4° with an interval of 1° for each simulation. For ease of analysis, samples of flap angle 4° and -4° were taken. At flap deflection $\delta_f = 4^\circ$, the boat moves to the Northwest. This is because the sail as the main provider of force produces the lift force to the North and the drag force to the West so that the resultant force is generated to the Northwest. The free-body diagram at the beginning of the simulation of case II $\delta_f = 4^\circ$ and $\delta_r = 0^\circ$ is shown in Figure 9.

It can be seen that the boat rotates counter-clockwise so that ψ is negative, and the boat moves to the negative x -axis

and positive y-axis, or the Northwest at global coordinates, as shown in Figure 10.

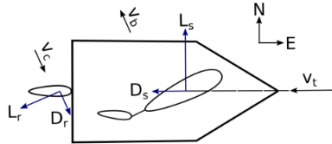


Fig. 9. Free-body diagram at the beginning of case II $\delta_f = 4^\circ$ and $\delta_r = 0^\circ$

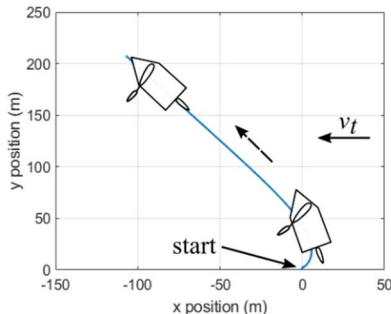


Fig. 10. Boat movement in case II, $\delta_f = 4^\circ$ dan $\delta_r = 0^\circ$

The resultant of boat velocity in case II $\delta_f = 4^\circ$ and $\delta_r = 0^\circ$ reaches a maximum value of 3.3 m/s and is constant at that value until the simulation ended. The direction boat velocity at the beginning of the simulation is at angle -114° which means to the right and the rear corner of the boat, then goes up to the angle of 0° which means to the front of the boat and is constant until the end of the simulation. For the flap and rudder deflections $\delta_f = -4^\circ$ and $\delta_r = 0^\circ$, the result will be symmetrical results being mirrored to the x-axis.

C. Case III

In case III, rudder deflection $\delta_r = 15^\circ$ and flap deflection $\delta_f = 4^\circ$. Because $\delta_f = 4^\circ$, the wing sail angle of attack $\alpha_s = 12.8^\circ$ is formed and the lift force (L_s) is generated to the north and drag (D_s) to the West which moves the boat to the Northwest at the beginning of the simulation. The rudder that deflects $\delta_r = 15^\circ$ also produces lift (L_r) and drag (D_r) forces from the relative motion between the rudder and seawater. The free- body diagram at the beginning of case IV $\delta_f = 4^\circ$ and $\delta_r = 15^\circ$ is shown in Figure 11.

In this case, the boat moves toward the negative x-axis and positive y-axis direction of global coordinates, as shown in Figure 12. The boat rotates counter-clockwise at global coordinates until it is constant at an angle of 5° .

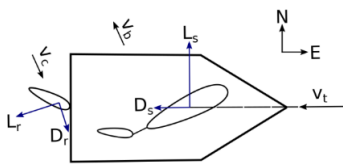


Fig. 11. Free-body diagram at the beginning of case IV $\delta_f = 4^\circ$ dan $\delta_r = 15^\circ$

The magnitude of boat velocity in this case reaches a maximum value of 1.4 m/s at 29 seconds then reaches constant at 67 seconds with a value of 0.67 m/s. At the beginning the direction of the boat velocity is at an angle of -121° or to the left rear of the boat due to the dominant wing sail force. After 4 seconds the velocity direction shifts and reaches constant at 59 seconds with an angle of 15° or towards the right front of the boat. For rudder and flap deflection $\delta_r = -15^\circ$ and $\delta_f = -4^\circ$ shows symmetrical results being mirrored to the x-axis.

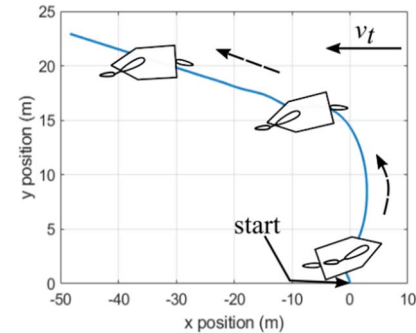


Fig. 12. Boat movement in case IV $\delta_r = 15^\circ$ dan $\delta_f = 4^\circ$

D. Case IV

In case IV, along the simulation rudder deflection $\delta_r = -15^\circ$ and flap deflection $\delta_f = 4^\circ$. Because $\delta_f = 4^\circ$, the wing sail angle of attack $\alpha_s = 12.8^\circ$ is formed and the lift force (L_s) is generated to the North and drag (D_s) to the West by the wing sail which moves the boat to the Northwest at the beginning of the simulation. The rudder that deflects $\delta_r = -15^\circ$ also produces lift (L_r) and drag (D_r) forces due to the relative motion between the rudder and seawater. The free- body diagram at the beginning of the simulation case V with $\delta_f = 4^\circ$ and $\delta_r = -15^\circ$ is shown in Figure 13.

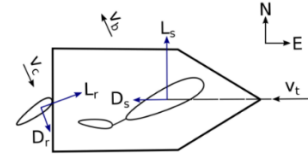


Fig. 13. Free-body diagram at the beginning of case V $\delta_f = 4^\circ$ and $\delta_r = -15^\circ$

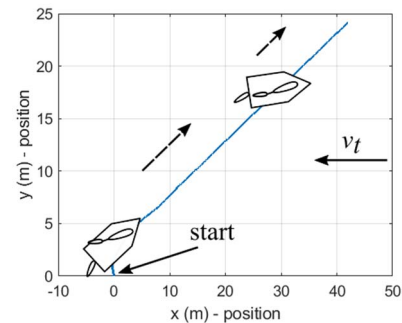


Fig. 14. Boat movement in case V $\delta_r = -15^\circ$ and $\delta_f = 4^\circ$

Figure 14 shows that the boat is moving in the positive x and y axes or in the Northeast direction. The boat rotates counter-clockwise on the global Z axis which means the value ψ is negative until the 59th second ψ constant at an angle of -12° .

The boat reaches maximum velocity at 18 seconds at 0.65 m/s and reaches a constant condition at 59 seconds with a

magnitude of 0.53 m/s. At the beginning of the simulation the boat velocity direction reaches the angle of -109° and gradually shifts to a constant condition of the speed of the boat at an angle of -15° or towards the left front corner of the boat. For rudder and flap deflections $\delta_r = 15^\circ$ and $\delta_f = -4^\circ$ the result will be symmetrical being mirrored to the x-axis.

E. Case V

In the case V, the flap and rudder deflections are set with square wave input with a frequency of 0.1 rad/s or 0.016 Hz and then filtered with the transfer function $\frac{1}{s+1}$. Flaps with deflection angles of 4° and -4° and rudder with deflection angles of -15° and 15° , as shown in Figure 17. The free-body diagram at the beginning of the simulation of this case is the same as the free-body diagram at the beginning of the case IV simulation shown in Figure 14.

From Figure 16 it can be seen that the boat moves zigzag towards the East. In sailing terms this movement is known as tacking, which is the movement of the boat upwind. Boat yaw movements (ψ) up and down with a maximum value of -30° and 27° . First the boat rotates counter-clockwise at global coordinates then when the flap and rudder deflection changes the boat begins to rotate clockwise.

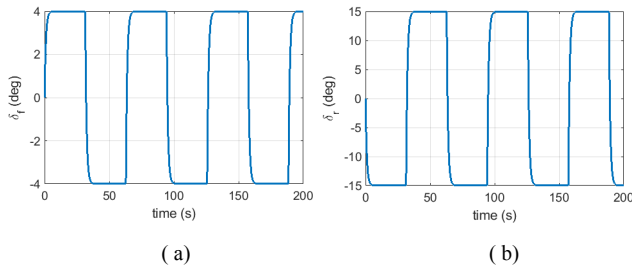


Fig. 15. Deflection of (a) flap and (b) rudder in case V tacking $\delta_r = -15^\circ \rightarrow 15^\circ$ and $\delta_f = 4^\circ \rightarrow -4^\circ$

The resultant boat velocity reaches a maximum value of 0.65 m/s at the beginning of the simulation, and the velocity decreases with each deflection change. When the velocity is steady, the velocity direction is at an angle of 47.5° .

Tacking simulation with the opposite input to case V where δ_f starts from -4° then 4° and δ_r starts from 15° then -15° ($\delta_f = -4^\circ \rightarrow 4^\circ$ and $\delta_r = 15^\circ \rightarrow -15^\circ$) shows symmetrical results with simulation case V $\delta_f = 4^\circ \rightarrow -4^\circ$ and $\delta_r = -15^\circ \rightarrow 15^\circ$. The plot of the boat's movement is shown in Figure 16.

IV. DEVELOPMENT OF CONTROL SYSTEM

After having the dynamic model of the sailboat, it is time to consider the options for controlling the motion of the boat available in the literature. Benoit Clement in Reference [8] discusses a simple control strategy in embedded systems with the Hardware in the Loop (HIL) methodology. The approach taken is to navigate the sailboat by following the line strategy (line following strategy) by controlling the rudder and sail.

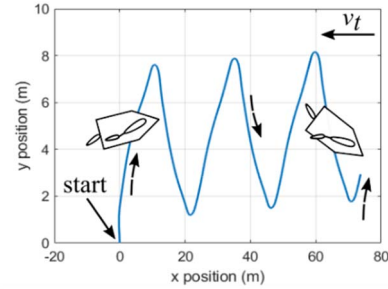


Fig. 16. Boat movement in case V tacking $\delta_r = -15^\circ \rightarrow 15^\circ$ and $\delta_f = 4^\circ \rightarrow -4^\circ$

In the Reference article [4], Andouglas G. S. Júnior et al discuss the autonomous sailboat control architecture with mathematical models using PID and Fuzzy controllers to control sail and rudder in closed-loop control systems. The control hardware used is Arduino and Raspberry PI. The values of the K_p , K_i , and K_d parameters are obtained from the tune of the Matlab software. Whereas the fuzzy logic used has two inputs (the orientation error and its derivative), and the output will be the angle of the screen, that is, how tight or tight the rope must sail.

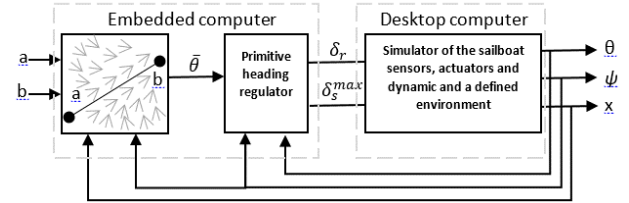


Fig. 17. HIL architecture for autonomous sailboat

In addition, in the B. Puviyarasi study [5], building a non-linear autonomous sailboat control system is carried out using a Conventional PID controller (CPID) and Adaptive PID controller (APID). The difference between CPID and APID is the tuning process. The tuning process on the APID for sailboats is done automatically using Matlab software. A comparison of CPID and APID produces data that shows that the Adaptive PID controller provides more stable control.

In other work, dos-Santos in [10] proposes a navigation system that allows a sailboat to reach the desired target point in its work environment. This navigation system consists of a low-level canopy controller and a short-term track planner for situations against the wind. For low-level canopy controllers, the proportional-integral gain-scheduling controller (GS-PI) is shown to better illustrate the nonlinear motion inherent in sailboat movements. Gain-scheduling-PI consists of tables containing the best control parameters learned and determined for a particular maneuver and scheduling according to each situation. The idea is to design special controllers that meet the specific control objectives of each application. Changes in proportional and integral parameters modify the behavior of the steering wheel and consequently affect the movement of the sailboat. The experiment to find the GS-PI controller is similar to the static PI, but the experiment is applied to some wind direction and initial sailboat orientation. The strategy for finding the GS-PI controller introduced in this study can be automated using a sailboat mathematical model. The main drawback to the design of the GS-PI controller is to find a suitable model that represents the movement of the sailboat.

The study of Silva-Junior in [11] discusses autonomous sailboat control with a learning reinforcement approach (Q-Learning). The Q-Learning approach is used based on a reward matrix and a series of actions that change in the direction of the wind to take into account dead zones, which are areas against the wind where the sailboat cannot gain speed.

The control architecture is arranged at a low level consisting of heading and propulsion controls, which work independently. Propulsion control changes sail position so that the sailboat has a forward speed according to the current wind speed and direction. The heading control changes the position of the rudder so the sailboat can follow the line connecting the last and upcoming waypoints. At a higher level, there are local and global path planning modules. Local lane planning uses information about surface and underwater obstacles to find alternative routes to avoid it. Global path planning uses information about climate and terrain to find suitable routes for N-boats. The basic processing flow of the N-boat Q-Learning algorithm is to create a simplified terrain map to obtain a discrete description of the environment. Next, a wind map is seen to get its direction and to erase actions that place the N-boat inside the dead zone, so that a safe path can be studied. Finally, the algorithm is trained so that a safe and feasible path is found and passed on to the other lower layers.

One study by Abrougui in [12] discusses controlling a sailboat with two or three hulls by developing a backstepping method. The backstepping method was developed to stabilize the canopy of the boat while tracking waypoints. The basic idea behind this method is to break down the full system design problem into a sequence of sub-problems on a low-level system, and recursively use several statements as "virtual inputs" to obtain intermediate control laws with the Control Lyapunov Function (CLF). According to Abrougui, the main advantage of backstepping control is the guarantee of system stability.

Viel in [13] discusses the method of sailboat reaching the target area, stopping at the target area, and returning to the target area when the wind makes the sailboat come out. This system consists of 3 steps, namely step 1: Direct path, which is determining the shorter path to the target, Step 2: Go round the target, Step 3: Tack strategy, which is a tactic to move against the wind, Step 4: Upwind strategy that is when the sailboat is in the target area, the sailboat should move as little as possible to direct the ship in the direction of the wind.

For future work, this study will develop the most straightforward control algorithm for implementation. However, during simulation in Matlab/Simulation environment, all of the performance of the mentioned control methods will be analyzed for many scenarios in which the dynamic model developed in this study can be very useful.

V. CONCLUSION

The Analysis and Simulation of Wing sail Autonomous Boat Dynamics have been carried out, and conclusions have been obtained. In the flap deflection range of -4° to 4° with $\delta_f = 0^\circ$, the speed of the boat increases with the increase of the flap deflection angle. In the rudder deflection range of -15° to

15° with $\delta_r = 0^\circ$, the speed of the boat decreases as the rudder deflection angle rises. Inputs $\delta_f = 4^\circ$ and $\delta_r = 15^\circ$ cause the boat to move to the Northwest, and inputs $\delta_f = 4^\circ$ and $\delta_r = -15^\circ$ cause the boat to move to the Northeast. The wing sail autonomous boat can maneuver tacking to sail upwind with square wave input, flap deflection values 4° and -4° and rudder -15° and 15° , and frequency of 0.1 rad/s. For the opposite deflection input, the simulation shows symmetrical results. In overall there are four direction-combinations of the flap and rudder motions such that the sailboat can be steered as desired. The autonomous boat dynamics simulation model that has been made can be used to develop flap and rudder control algorithms. Several potential methods to control the autonomous sailboat is discussed. Future work will include the control design and simulation in Matlab/Simulink environment, HIL simulation, and implementation of the control system to the sailboat prototype.

ACKNOWLEDGMENT

This paper was partially supported by the Directorate of Research and Community Service, Ministry of Research, Technology and Higher Education Fiscal Year 2020, and the USAID through Sustainable Higher Education Research Alliances (SHERA) Program-Centre for Collaborative Research (CCR) National Center for Sustainable Transportation Technology (NCSTT).

REFERENCES

- [1] J. Alves, T. Ramos, and N. Cruz, "A reconfigurable computing system for an autonomous sailboat," in *International Robotic Sailing Conference*, 2008, pp. 13–20.
- [2] C. Tretow, "Design of a free-rotating wing sail for an autonomous sailboat," KTH Royal Institute of Technology, 2017.
- [3] Legursky, K, "System Identification And The Modeling Of Sailing Yachts," University of Kansas, 2017.
- [4] Y. A. Cengel and J. M. Cimbala, *Fluid Mechanics*, 1st ed. New York: McGraw-Hill, 2006.
- [5] L. Du, A. Berson, and R. G. Dominy, "Aerofoil behaviour at high angles of attack and at Reynolds numbers appropriate for small wind turbines," *Mech. Eng. Sci.*, vol. 0, pp. 1–16, 2014.
- [6] Fossen, T. I, "*Handbook of Marine Craft Hydrodynamics and Motion Control.*" West Sussex: John Wiley & Sons, 2011.
- [7] Clement, B. Control Algorithms for a Sailboat Robot with a Sea Experiment. IFAC Proceedings Volumes Volume 46, Issue 33, Pages 19-24. Elsevier, 2013.
- [8] Júnior, A.G., Gonçalves, L. M. G. and Aroca, R. V. N-BOAT: An Autonomous Robotic Sailboat. IEEE Latin American Robotics Symposium, 2013
- [9] Puviyarasi, B., Nithyaranji, N., Tamilselvi, T. and Srivady, K. Adaptive Pid Control Of An Autonomous Sailboat. International Journal of Engineering and Advanced Technology (IJEAT) ISSN: 2249 – 8958, Volume-8, Issue-6, August 2019.
- [10] dos-Santos, D. H. and Garcia-Goncalves, L. M. A gain-scheduling control strategy and short-term path optimization with genetic algorithm for autonomous navigation of a sailboat robot. International Journal of Advanced Robotic Systems : 1–15. Saga, 2019.
- [11] Silva-Junior, A. G., dos-Santos, D. H., de-Negreiros, A. P. F., Souza-Silva, J. M. V. B. and Garcia-Gonçalves, L. M. High-Level Path Planning for an Autonomous Sailboat Robot Using Q-Learning. Sensors, 20. MDPI, 2020.
- [12] Abrougui, H. and Nejim, S. Backstepping Control of an Autonomous Catamaran Sailboat. Robotic Sailing, 2018.
- [13] Viel, C., Vautier, U., Wan, J. and Jaulin, L. Position Keeping Control of an Autonomous Sailboat. IFAC-PapersOnLine Volume 51, Issue 29, 2018, Pages 14-19. Elsevier, 2018.